J|A|C|S ARTICLES

Published on Web 06/25/2010

Control of the Orientational Order and Nonlinear Optical Response of the "Push−Pull" Chromophore RuPZn via Specific Incorporation into Densely Packed Monolayer Ensembles of an Amphiphilic 4-Helix Bundle Peptide: Second Harmonic Generation at High Chromophore Densities

Grazia Gonella,*[,†] Hai-Lung Dai,[†] H. Christopher Fry,[‡] Michael J. Therien,[§] Venkata Krishnan,[‡] Andrey Tronin,[‡] and J. Kent Blasie*[,‡]

Department of Chemistry, Temple University, Philadelphia, Pennsylvania 19122, Department of Chemistry, University of Pennsylvania, Philadelphia, Pennsylvania 19104, and Department of Chemistry, Duke University, Durham, North Carolina 27708

Received February 5, 2010; E-mail: gonella@temple.edu; jkblasie@sas.upenn.edu

Abstract: The macroscopic nonlinear optical response of the "push−pull" chromophore **RuPZn** incorporated into a single monolayer of the amphiphilic 4-helix bundle peptide (**AP0**) covalently attached to a solid substrate at high in-plane density has been measured. The second-order susceptibility, χ_{zzz}, was found to be in the range of $\sim 15 \times 10^{-9}$ esu, consistent with a coherent sum of the nonlinear contributions from the individual chromophores ($\vec{\beta}$) as previously measured in isotropic solution through hyper-Rayleigh scattering as well as estimated from theoretical calculations. The microscopic hyperpolarizability of the **RuPZn** chromophore is preserved upon incorporation into the peptide monolayer, suggesting that the chromophore−chromophore interactions in the densely packed ensemble do not substantially affect the first-order molecular hyperpolarizability. The polarization angle dependence of the second harmonic signal reveals that the chromophore is vectorially oriented in the two-dimensional ensemble. Analysis of the order parameter together with information obtained from grazing incidence X-ray diffraction help in determining the chromophore orientation within the **AP0**−**RuPZn** monolayer. Taking into account an average pitch angle of $\sim 20°$ characterizing the coiled-coil structure of the peptide bundle, the width of the bundle's tilt angle distribution should be $\sigma \leq 20°$, resulting in a mean value of the tilt angle $23° \leq \theta_0 \leq 37°$.

I. Introduction

Many chromophores that feature large dynamic hyperpolarizabilities (β_λ values) exploit a highly polarizable porphyrinic component.[1−22] Of these porphyrin-based high β_λ chromophores, the structures that possess the most spectacular hyperpolarizabilities feature (porphinato)zinc(II) (**PZn**) and metal(II)polypyridyl (**M**) units linked via an ethyne bridge (**M**−**PZn** species); this mode of chromophore-to-chromophore connectivity effectively mixes the **PZn** $\pi-\pi^*$ and metal polypyridyl-based

† Temple University.
‡ University of Pennsylvania.
§ Duke University.

(1) LeCours, S. M.; DiMagno, S. G.; Therien, M. J. *J. Am. Chem. Soc.* **1996**, *118*, 11854.
(2) LeCours, S. M.; Guan, H.-W.; DiMagno, S. G.; Wang, C. H.; Therien, M. J. *J. Am. Chem. Soc.* **1996**, *118*, 1497.
(3) Priyadarshy, S.; Therien, M. J.; Beratan, D. N. *J. Am. Chem. Soc.* **1996**, *118*, 1504.
(4) Karki, L.; Vance, F. W.; Hupp, J. T.; LeCours, S. M.; Therien, M. J. *J. Am. Chem. Soc.* **1998**, *120*, 2606.
(5) Shediac, R.; Gray, M. H. B.; Uyeda, H. T.; Johnson, R. C.; Hupp, J. T.; Angiolillo, P. J.; Therien, M. J. *J. Am. Chem. Soc.* **2000**, *122*, 7017.
(6) Screen, T. E. O.; Thorne, J. R. G.; Denning, R. G.; Bucknall, D. G.; Anderson, H. L. *J. Am. Chem. Soc.* **2002**, *124*, 9712.
(7) Uyeda, H. T.; Zhao, Y. X.; Wostyn, K.; Asselberghs, I.; Clays, K.; Persoons, A.; Therien, M. J. *J. Am. Chem. Soc.* **2002**, *124*, 13806.
(8) Rubtsov, I. V.; Susumu, K.; Rubtsov, G. I.; Therien, M. J. *J. Am. Chem. Soc.* **2003**, *125*, 2687.
(9) Drobizhev, M.; Stepanenko, Y.; Dzenis, Y.; Karotki, A.; Rebane, A.; Taylor, P. N.; Anderson, H. L. *J. Phys. Chem. B* **2005**, *109*, 7223.
(10) Susumu, K.; Duncan, T. V.; Therien, M. J. *J. Am. Chem. Soc.* **2005**, *127*, 5186.
(11) Zhang, T.-G.; Zhao, Y.; Asselberghs, I.; Persoons, A.; Clays, K.; Therien, M. J. *J. Am. Chem. Soc.* **2005**, *127*, 9710.
(12) Duncan, T. V.; Susumu, K.; Sinks, L. E.; Therien, M. J. *J. Am. Chem. Soc.* **2006**, *128*, 9000.
(13) Zhang, T.-G.; Zhao, Y.; Song, K.; Asselberghs, I.; Persoons, A.; Clays, K.; Therien, M. J. *Inorg. Chem.* **2006**, *45*, 9703.
(14) Duncan, T. V.; Ishizuka, T.; Therien, M. J. *J. Am. Chem. Soc.* **2007**, *129*, 9691.
(15) Hisaki, I.; Hiroto, S.; Kim, K. S.; Noh, S. B.; Kim, D.; Shinokubo, H.; Osuka, A. *Angew. Chem. Int. Ed.* **2007**, *46*, 5125.
(16) Duncan, T. V.; Song, K.; Hung, S.-T.; Miloradovic, I.; Nayak, A.; Persoons, A.; Verbiest, T.; Therien, M. J.; Clays, K. *Angew. Chem. Int. Ed.* **2008**, *47*, 2978.
(17) Keinan, S.; Therien, M. J.; Beratan, D. N.; Yang, W. *J. Phys. Chem. A* **2008**, *112*, 12203.
(18) Song, J.; Jang, S. Y.; Yamaguchi, S.; Sankar, J.; Hiroto, S.; Aratani, N.; Shin, J.-Y.; Easwaramoorthi, S.; Kim, K. S.; Kim, D.; Shinokubo, H.; Osuka, A. *Angew. Chem. Int. Ed.* **2008**, *47*, 6004.
(19) Thorley, K. J.; Hales, J. M.; Anderson, H. L.; Perry, J. W. *Angew. Chem. Int. Ed.* **2008**, *47*, 7095.
(20) Reeve, J. E.; Collins, H. A.; Mey, K. D.; Kohl, M. M.; Thorley, K. J.; Paulsen, O.; Clays, K.; Anderson, H. L. *J. Am. Chem. Soc.* **2009**, *131*, 2758.
(21) Therien, M. J. *Nature* **2009**, *458*, 716.
(22) Hu, X.; Xiao, D.; Keinan, S.; Asselberghs, I.; Therien, M. J.; Clays, K.; Yang, W.; Beratan, D. N. *J. Phys. Chem. C* **2010**, *114*, 2349.

charge-resonance absorption oscillator strength and aligns the respective charge transfer transition dipoles of these building blocks along the highly conjugated molecular axis.[7,15−17,22] These structures exhibit extensive interpigment electronic interactions, display unusual dependence of the sign and magnitude of hyperpolarizability on incident irradiation frequency, and manifest extraordinarily large β_λ values at telecommunication-relevant wavelengths.

In order to optimize the macroscopic properties of ensembles of chromophores in the solid state, control of the ordering and intermolecular interactions is of utmost importance.[23−25] Various strategies have been followed to realize the theoretically predicted ensemble properties. For example, incorporation of nonlinear optical (NLO) chromophores into a polymeric matrix where orientational order is achieved by "poling" with a strong external dc electric field (for an exhaustive review see Cho et al.[26] and references therein) and Langmuir−Blodgett deposition of NLO−chromophore monolayer and multilayer films[27−30] are traditional methods by which macroscopic processable NLO materials have been fabricated.

The method chosen in this study to transfer the microscopic properties of the chromophore to a macroscopic scale is yet a different one: it is based on the utilization of an amphiphilic 4-helix bundle peptide (**AP0**), which is able to specifically bind the metal ion of the porphyrinic component of the chromophore we utilize through axial hystidyl ligation (at position 6).[31−33] In this report, we examine the macroscopic ordering, packing, and nonlinear polarizability of an archetypal member of the **MPZn** chromophore family, ruthenium(II) [5-(4′-ethynyl-(2,2′;6′,2″-terpyridinyl))-10,20-bis(phenyl)porphinato]-zinc(II)-(2,2′;6′,2″-terpyridine)$^{2+}$ (**RuPZn**)[7] bound within the amphiphilic **AP0** peptide (Scheme 1). The amphiphilicity of **AP0** enables the vectorial orientation of the **RuPZn**−**AP0** complex in macroscopic ensembles at the water−gas interface, with the long axis of the bundle perpendicular to the interface when high surface pressures are applied. Chemical specificity designed into either end of the bundle enables the covalent attachment of this monolayer onto the surface of an opportunely prepared inorganic substrate such as fused silica. Structural studies on monolayers of these complexes at the air−water interface[31,32] and on solid substrates[34] indicate that it is possible to obtain very high density and good ordering of the hyperpolarizable peptide chromophores: the two key ingredients of this fabrication method for the translation of the promising NLO properties of the chromophores onto a macroscopic scale.

Scheme 1. Schematic Representation of the (a) Amino Acid Sequence[a] for **AP0**, (b) **RuPZn**, (c) the 4-Helix Bundle,[b] and (d) the **AP0**−**RuPZn** Complex[c]

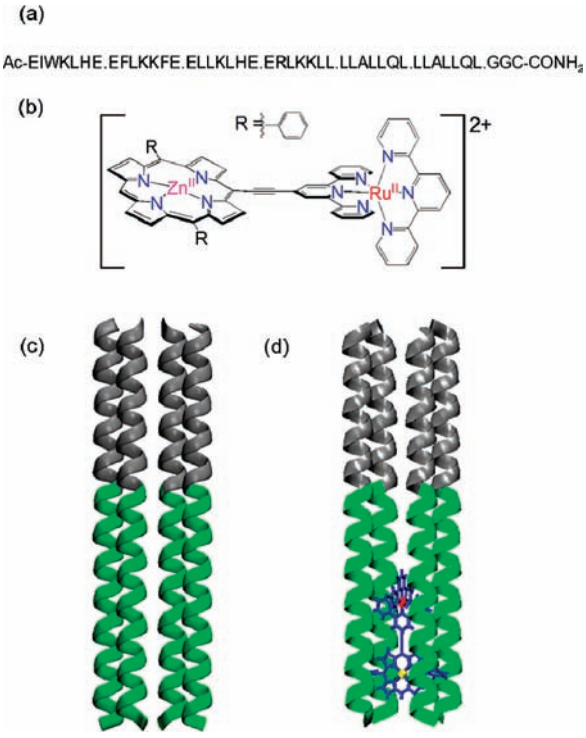

[a] One letter symbol. [b] The α-helices are shown in the ribbon representation, green and gray representing the hydrophilic and hydrophobic domains, respectively. [c] The Zn and Ru atoms are represented in yellow and red, respectively (for further details see ref 34). Proof of such a unique vectorial orientation of the chromophore within the bundle is provided in this paper.

In order to ascertain that the exceptional NLO properties of the chromophore are preserved on the macroscopic scale in the new material, second harmonic generation (SHG) measurements are utilized.[30,35−37] SHG is generated wherever the inversion symmetry is broken: this can be the case, for instance, at the interface between two centrosymmetric media or in a monolayer of oriented molecules. In the latter case, the SH intensity can be enhanced if the fundamental and/or second harmonic wavelengths coincide with an appropriate molecular electronic transition. By using selected polarization combinations, the relative magnitude of the susceptibility elements can be determined and, furthermore, by comparison with the signal from a well-known reference such as quartz, the absolute value of the elements of the second-order susceptibility $\vec{\vec{\chi}}^{(2)}$ tensor of the material can be measured.

In this work we investigate the SH response of **RuPZn** chromophores incorporated in a high-density **AP0** monolayer deposited on a fused silica substrate. In particular, we deduce

(23) Kuzyk, M. G.; Singer, K. D.; Zahn, H. E.; King, L. A. *J. Opt. Soc. Am. B* **1989**, *6*, 742.
(24) Risser, S. M.; Beratan, D. N.; Marder, S. R. *J. Am. Chem. Soc.* **1993**, *115*, 7719.
(25) Harper, A. W.; Sun, S.; Dalton, L. R.; Garner, S. M.; Chen, A.; Kalluri, S.; Steier, W. H.; Robinson, B. H. *J. Opt. Soc. Am. B* **1998**, *15*, 329.
(26) Cho, M. J.; Choi, D. H.; Sullivan, P. A.; Akelaitis, A. J. P.; Dalton, L. R. *Prog. Polym. Sci.* **2008**, *33*, 1013.
(27) Dalton, L. R.; Harper, A. W.; Ghosn, R.; Steier, W. H.; Ziari, M.; Fetterman, H.; Shi, Y.; Mustacich, R. V.; Jen, A. K. Y.; Shea, K. J. *Chem. Mater.* **1995**, *7*, 1060.
(28) Marks, T. J.; Ratner, M. A. *Angew. Chem. Int. Ed.* **1995**, *34*, 155.
(29) Halter, M.; Liao, Y.; Plocinik, R. M.; Coffey, D. C.; Bhattacharjee, S.; Mazur, U.; Simpson, G. J.; Robinson, B. H.; Keller, S. L. *Chem. Mater.* **2008**, *20*, 1778.
(30) Leray, A.; Leroy, L.; Le Grand, Y.; Odin, C.; Renault, A.; Vie, V.; Rouede, D.; Mallegol, T.; Mongin, O.; Werts, M. H. V.; Blanchard-Desce, M. *Langmuir* **2004**, *20*, 8165.
(31) Xu, T.; Wu, S. P.; Miloradovic, I.; Therien, M. J.; Blasie, J. K. *Nano Lett.* **2006**, *6*, 2387.
(32) Strzalka, J.; Xu, T.; Tronin, A.; Wu, S. P.; Miloradovic, I.; Kuzmenko, I.; Gog, T.; Therien, M. J.; Blasie, J. K. *Nano Lett.* **2006**, *6*, 2395.
(33) Zou, H. L.; Therien, M. J.; Blasie, J. K. *J. Phys. Chem. B* **2008**, *112*, 1350.
(34) Krishnan, V.; Tronin, A.; Strzalka, J.; Fry, H. C.; Therien, M. J.; Blasie, J. K. Submitted for publication, 2010.
(35) Reyes-Esqueda, J.; Darracq, B.; Garcia-Macedo, J.; Canva, M.; Blanchard-Desce, M.; Chaput, F.; Lahlil, K.; Boilot, J. P.; Brun, A.; Levy, Y. *Opt. Commun.* **2001**, *198*, 207.
(36) Fujii, S.; Morita, T.; Kimura, S. *J. Pept. Sci.* **2008**, *14*, 1295.
(37) Li, Z. A.; Wu, W. B.; Yu, G.; Liu, Y. Q.; Ye, C.; Qin, J. G.; Li, Z. *ACS Appl. Mater. Interfaces* **2009**, *1*, 856.

from the SHG measurements the absolute magnitude of the second-order susceptibility of the ensemble and the orientation of the chromophore molecules in the monolayer.

II. Second Harmonic Generation from a Two-Dimensional Ensemble

In our experiment, the SH intensity at a particular polarization measured as a function of the fundamental polarization angle was analyzed to obtain information about the second-order susceptibility of the monolayer as well as the orientation of the **RuPZn** chromophores within the monolayer itself. For an achiral monolayer of molecules distributed randomly on the surface (*xz* plane) the third-rank second-order susceptibility tensor $\vec{\vec{\chi}}^{S}$ has only four unique nonzero elements that reduce to three in the case of SHG: χ_{zzz}, $\chi_{zxx} = \chi_{zyy}$ and $\chi_{xzx} = \chi_{xxz} = \chi_{yzy} = \chi_{yyz}$.[38]

In the experimental configuration a $\lambda/2$ plate has been used to control the input polarization angle γ such that the *p* and *s* components of the incident electric field can be defined as

$$\begin{aligned} E_p(\omega) &= E(\omega)\cos\gamma \\ E_s(\omega) &= E(\omega)\sin\gamma \end{aligned} \tag{1}$$

with $\gamma = 0$ ($\pi/2$) for purely *p*(*s*)-polarized fundamental light, where *p*(*s*)-polarized light refers to the electric field with polarization parallel (perpendicular) to the plane of incidence. The measured *p*- and *s*-polarized SH intensity can be expressed as a function of the polarization of the fundamental as

$$\begin{aligned} I_p(2\omega) &\propto |\chi^{\mathrm{eff}}_{ppp}\cos^2\gamma + \chi^{\mathrm{eff}}_{pss}\sin^2\gamma|^2 I^2(\omega) \\ I_s(2\omega) &\propto |\chi^{\mathrm{eff}}_{sps}\sin\gamma\cos\gamma|^2 I^2(\omega) \end{aligned} \tag{2}$$

where $I(\omega)$ is the intensity of the fundamental beam. Note that in eq 2 instead of the susceptibility tensor $\vec{\vec{\chi}}^{S}$, the $\vec{\vec{\chi}}^{S,\mathrm{eff}}$ tensor, known as the effective susceptibility tensor, has been used. The elements of these two tensors are related through the Fresnel coefficients, c_{ijk}, by the following expressions:

$$\begin{aligned} \chi^{\mathrm{eff}}_{ppp} &= 2c_{xzx}\chi_{xzx} + c_{zxx}\chi_{zxx} + c_{zzz}\chi_{zzz} \\ \chi^{\mathrm{eff}}_{pss} &= c_{zyy}\chi_{zxx} \\ \chi^{\mathrm{eff}}_{sps} &= 2c_{yzy}\chi_{xzx} \end{aligned} \tag{3}$$

The coefficients c_{ijk} in eq 3 represent, as usual in the treatment of SHG from thin films or surfaces,[39] combinations of linear and nonlinear Fresnel factors depending upon the experimental geometry. In the literature, several models have been used to describe the reflected and transmitted electric field in the presence of a thin nonlinear film: they differ mainly for the choice of the Fresnel factors.[40−44] The values of c_{ijk} coefficients for our experimental configuration can be calculated by using a treatment similar to the one reported for SH measurement in reflection geometry by Simpson et al.,[44] which takes into account the multiple reflections of both fundamental and SH light inside the thin monolayer. We model our sample as a four-media system as shown in Figure 1: medium 1 is a semi-infinite linear medium representing the external environment on the incidence side, medium 2 is the substrate, medium 3 is the thin nonlinear film medium of thickness $d = 6.3$ nm, which is much smaller than the wavelength λ, and the fourth medium is another semi-infinite linear medium representing the external environment on the transmission side. We denote the refractive indexes of the media (in general represented by complex quantities) as n_x^{Ω} ($x = 1, 2, 3$ and $\Omega = \omega, 2\omega$) and they are assumed to be isotropic. In our experiment, medium 1 is air, medium 3 the peptide monolayer supporting the **RuPZn** chromophores, and medium 2 the amorphous silica slab alkylated on both surfaces.[34]

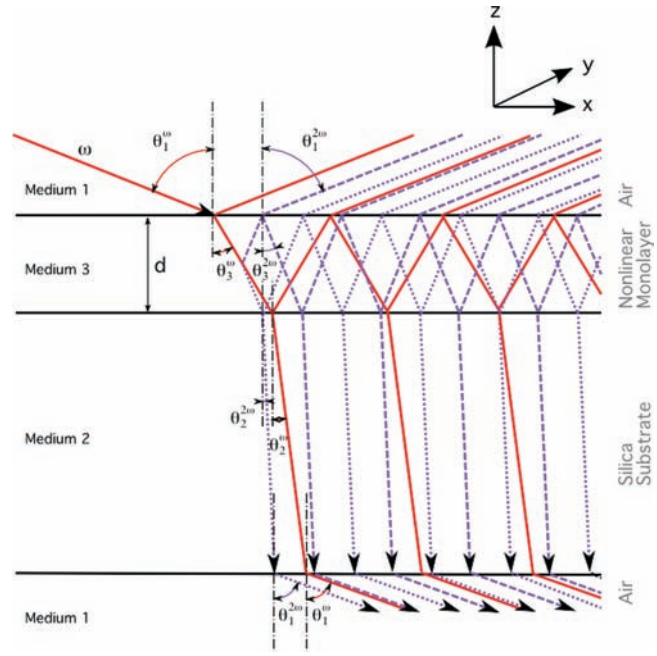

Figure 1. Schematic diagram (not to scale) describing the propagation of the fundamental (red) and SH waves (purple) through the four-media sample.

The c_{ijk} coefficients in eq 1 can then be expressed as

$$\begin{aligned} c_{xzx} &= L^{2\omega}_{xx}\cos\theta^{2\omega}_1 L^{\omega}_{zz}\sin\theta^{\omega}_3 L^{\omega}_{xx}\cos\theta^{\omega}_3 \\ c_{zxx} &= L^{2\omega}_{zz}\sin\theta^{2\omega}_1 (L^{\omega}_{xx}\cos\theta^{\omega}_3)^2 \\ c_{zzz} &= L^{2\omega}_{zz}\sin\theta^{2\omega}_1 (L^{\omega}_{zz}\sin\theta^{\omega}_3)^2 \\ c_{zyy} &= L^{2\omega}_{zz}\sin\theta^{2\omega}_1 (L^{\omega}_{yy})^2 \\ c_{yzy} &= L^{2\omega}_{yy} L^{\omega}_{zz}\sin\theta^{\omega}_3 L^{\omega}_{yy} \end{aligned} \tag{4}$$

where $\theta^{2\omega}_1$ defines the angle of the SH wave in air, while θ^{ω}_3 is the angle of the fundamental in the monolayer. These angles are related to the incidence angle of the fundamental wave, θ^{ω}_1, through the boundary conditions: $n^{\omega}_1 \sin\theta^{\omega}_1 = n^{2\omega}_1 \sin\theta^{2\omega}_1 = n^{\omega}_3 \sin\theta^{\omega}_3$.

The L^{Ω} ($\Omega = \omega, 2\omega$) coefficients, known as Fresnel factors for SHG, have the form

(38) Dick, B. *Chem. Phys.* **1985**, *96*, 199.
(39) Shen, Y. R. *The Principles of Nonlinear Optics* Wiley-Interscience: Hoboken, NJ, 2003; Chapter 25 (Surface Nonlinear Optics).
(40) Mizrahi, V.; Sipe, J. E. *J. Opt. Soc. Am. B* **1988**, *5*, 660.
(41) Zhang, T. G.; Zhang, C. H.; Wong, G. K. *J. Opt. Soc. Am. B* **1990**, *7*, 902.
(42) Feller, M. B.; Chen, W.; Shen, Y. R. *Phys. Rev. A* **1991**, *43*, 6778.
(43) Gruzdkov, Y. A.; Parmon, V. N. *J. Chem. Soc. Faraday Trans.* **1993**, *89*, 4017.
(44) Simpson, G. J.; Dailey, C. A.; Plocinik, R. M.; Moad, A. J.; Polizzi, M. A.; Everly, R. M. *Anal. Chem.* **2005**, *77*, 215.

$$
\begin{aligned}
L_{xx}^{\omega} &= \frac{t_{p13}^{\omega} e^{-i\beta^{\omega}/2}(1 - r_{p32}^{\omega} e^{-i\beta^{\omega}})}{1 - r_{p32}^{\omega} r_{p31}^{\omega} e^{-i2\beta^{\omega}}} \\
L_{yy}^{\omega} &= \frac{t_{s13}^{\omega} e^{-i\beta^{\omega}/2}(1 + r_{s32}^{\omega} e^{-i\beta^{\omega}})}{1 - r_{s32}^{\omega} r_{s31}^{\omega} e^{-i2\beta^{\omega}}} \\
L_{zz}^{\omega} &= \frac{t_{p13}^{\omega} e^{-i\beta^{\omega}/2}(1 + r_{p32}^{\omega} e^{-i\beta^{2\omega}})}{1 - r_{p32}^{2\omega} r_{p31}^{2\omega} e^{-i2\beta^{2\omega}}} \\
L_{xx}^{2\omega} &= \frac{t_{p32}^{2\omega} e^{-i\beta^{2\omega}/2}(1 - r_{p31}^{2\omega} e^{-i\beta^{2\omega}})}{1 - r_{p32}^{2\omega} r_{p31}^{2\omega} e^{-i2\beta^{2\omega}}} t_{p21}^{2\omega} \\
L_{yy}^{2\omega} &= \frac{t_{s32}^{2\omega} e^{-i\beta^{2\omega}/2}(1 + r_{s31}^{2\omega} e^{-i\beta^{2\omega}})}{1 - r_{s32}^{2\omega} r_{s31}^{2\omega} e^{-i2\beta^{2\omega}}} t_{s21}^{2\omega} \\
L_{zz}^{2\omega} &= \frac{t_{p32}^{2\omega} e^{-i\beta^{2\omega}/2}(1 + r_{p31}^{2\omega} e^{-i\beta^{2\omega}})}{1 - r_{p32}^{2\omega} r_{p31}^{2\omega} e^{-i2\beta^{2\omega}}} t_{p21}^{2\omega}
\end{aligned}
\tag{5}
$$

where $\beta^{\Omega} = (2\pi/\lambda^{\Omega}) n_3^{\Omega} d \cos\theta_3^{\Omega}$ indicates the phase thickness, and $r_{p(s)ij}^{\Omega}$ and $t_{p(s)ij}^{\Omega}$ are the Fresnel coefficients for reflection and transmission for $p(s)$-polarized light from medium i to medium j.[45] A detailed derivation of the L^{Ω} coefficients is provided in the Supporting Information.

The combination of eqs 2−5 enables the *p*- and *s*-polarized SHG intensities to be calculated as functions of the fundamental polarization. By fitting the experimentally measured polarization dependence, it is possible to obtain the susceptibility tensor elements χ_{ijk} in relative units and by comparison with the signal from a well-known reference, such as quartz, the χ_{ijk} elements can be expressed in absolute units. The χ_{ijk} elements, expressed in the laboratory macroscopic frame, can in turn be related to the components of the molecular first-order hyperpolarizability tensor, $\beta_{i'j'k'}$, in the reference frame of the molecule, by the following expression:

$$
\chi_{ijk} = N \sum_{i'j'k'} \langle R_{ii'} R_{jj'} R_{kk'} \rangle \beta_{i'j'k'} \tag{6}
$$

where N is the chromophore density, $R_{ll'}$ indicates the rotation matrix element between the macroscopic and the molecular reference frame, and the brackets denote the ensemble orientational average. The details of the orientational distribution of chromophores over the ensemble result for isotropic and centrosymmetric distributions of dipolar molecules in a value equal to zero, i.e., no macroscopic second-order response. Only narrow unimodal distributions result in a fully coherent response in which the individual molecular hypepolarizabilities ($\vec{\beta}$) interfere constructively summing to $N\vec{\beta}$. In Figure 2 the laboratory frame is related to the molecular frame through the orientation angles θ (tilt), φ (azimuth), and ξ (twist). Since the surface is isotropic with respect to the azimuthal angle φ (this result was proven experimentally by the absence of any change in the SH intensity measured upon rotation of the sample around the surface normal), eq 6 can be simplified by the integration over all the possible values that this angle can assume.

The hyperpolarizability tensor of the **RuPZn** chromophore, which shows pseudo-C_{2v} symmetry (with z' as a 2-fold axis), presents only five unique nonvanishing elements: $\beta_{z'z'z'}$, $\beta_{z'x'x'}$, $\beta_{z'y'y'}$, $\beta_{x'z'x'} = \beta_{x'x'z'}$, and $\beta_{y'z'y'} = \beta_{y'y'z'}$.[38] Note that the SH wavelength at 420 nm is known to be in resonance with a transition manifold having significant charge transfer character along the long molecular axis (z').[7] We can then consider in our treatment the following as major contributing components to the hyperpolarizability: $\beta_{z'z'z'}$, $\beta_{z'x'x'}$, and $\beta_{z'y'y'}$. Subsequently, the nonzero elements of the susceptibility tensor can be expressed using eq 6 as[46]

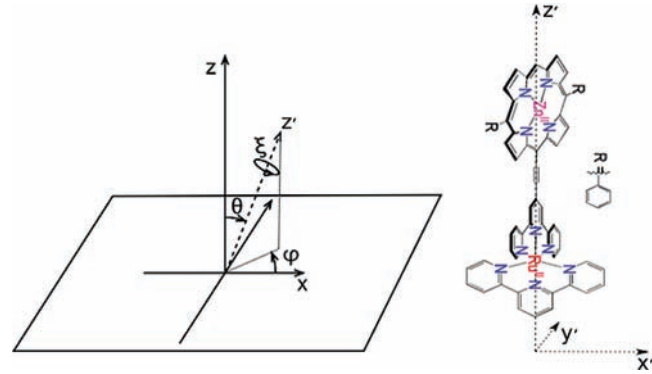

Figure 2. The macroscopic (laboratory) coordinates (x, y, z) and the microscopic (molecular) coordinates (x', y', z'). The direction cosines θ, φ, ξ define the relative orientation of the molecular coordinate system with respect to the laboratory coordinate system.

$$
\begin{aligned}
\chi_{zzz} &= N(\langle\cos^3\theta\rangle\beta_{z'z'z'} + \langle\sin^2\theta\cos\theta\sin^2\xi\rangle\beta_{z'y'y'} + \\
&\qquad \langle\sin^2\theta\cos\theta\cos^2\xi\rangle\beta_{z'x'x'}) \\
\chi_{zxx} &= \frac{1}{2}N(\langle\sin^2\theta\cos\theta\rangle\beta_{z'z'z'} - \langle\sin^2\theta\cos\theta\sin^2\xi\rangle\beta_{z'y'y'} - \\
&\qquad \langle\sin^2\theta\cos\theta\cos^2\xi\rangle\beta_{z'x'x'} + \langle\cos\theta\rangle(\beta_{z'x'x'} + \beta_{z'y'y'})) \\
\chi_{xzx} &= \frac{1}{2}N(\langle\sin^2\theta\cos\theta\rangle\beta_{z'z'z'} - \langle\sin^2\theta\cos\theta\sin^2\xi\rangle\beta_{z'y'y'} - \\
&\qquad \langle\sin^2\theta\cos\theta\cos^2\xi\rangle\beta_{z'x'x'})
\end{aligned}
\tag{7}
$$

In the case in which the twist angle ξ around the long molecular axis is broadly distributed, a reasonable assumption for an elongated molecule with C_{2v} symmetry, we can further average and simplify the above equations as

$$
\begin{aligned}
\chi_{zzz} &= N\left(\langle\cos^3\theta\rangle\beta_{z'z'z'} + \frac{1}{2}\langle\sin^2\theta\cos\theta\rangle(\beta_{z'x'x'} + \beta_{z'y'y'})\right) \\
\chi_{zxx} &= \frac{1}{2}N\left(\langle\sin^2\theta\cos\theta\rangle\left(\beta_{z'z'z'} - \frac{1}{2}(\beta_{z'x'x'} + \beta_{z'y'y'})\right) + \right. \\
&\qquad \left. \langle\cos\theta\rangle(\beta_{z'x'x'} + \beta_{z'y'y'})\right) \\
\chi_{xzx} &= \frac{1}{2}N\left(\langle\sin^2\theta\cos\theta\rangle\left(\beta_{z'z'z'} - \frac{1}{2}(\beta_{z'x'x'} + \beta_{z'y'y'})\right)\right)
\end{aligned}
\tag{8}
$$

Using eq 8 it is now possible to define the order parameter D, which is related to the orientation distribution of the tilt angle θ through[38]

$$
D \equiv \frac{\langle\cos^3\theta\rangle}{\langle\cos\theta\rangle} = \frac{\chi_{zzz} - \chi_{zxx} + \chi_{xzx}}{\chi_{zzz} - \chi_{zxx} + 3\chi_{xzx}} \tag{9}
$$

Similarly, from eq 8 we obtain the ratio

$$
\frac{\beta_{z'x'x'} + \beta_{z'y'y'}}{\beta_{z'z'z'}} = 2\frac{\chi_{zxx} - \chi_{xzx}}{\chi_{zzz} + 2\chi_{xzx}} \tag{10}
$$

(45) Azzam, R. M. A.; Bashara, N. M. *Ellipsometry and Polarized Light*; North-Holland−Elsevier Science Publishing Co., Inc.: Amsterdam, 1987.

(46) Moad, A. J.; Simpson, G. J. *J. Phys. Chem. B* **2004**, *108*, 3548.

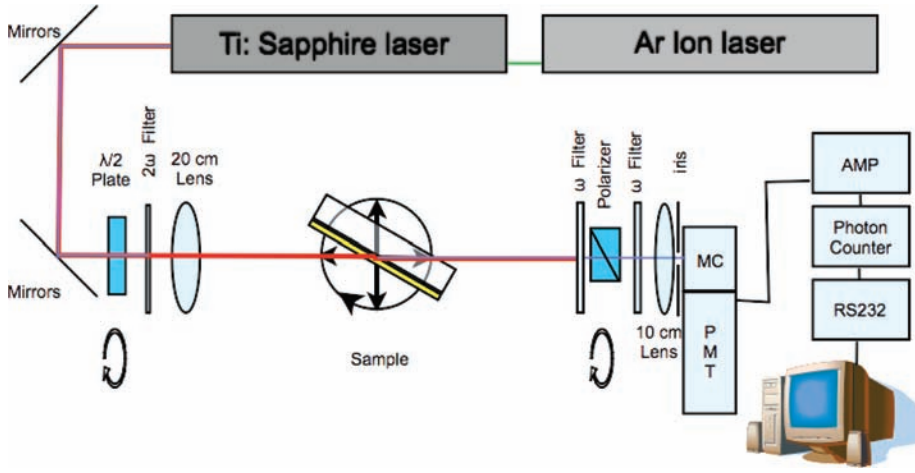

Figure 3. The diagram of the experimental setup for SHG experiments in transmission geometry.

In our analysis, we assume that the tilt angle orientation distribution is represented by a normalized, truncated Gaussian distribution $w(\theta) = 1/(2\pi\sigma)^{1/2} \exp[-(\theta - \theta_0)^2/2\sigma^2]$ centered at θ_0 with a standard deviation σ such as

$$\langle \cos^n \theta \rangle = \frac{\int_0^\pi w(\theta) \cos^n \theta \sin \theta \, d\theta}{\int_0^\pi w(\theta) \sin \theta \, d\theta}$$

III. Experimental Section

The samples were prepared and characterized as described in detail in ref 34. The SHG experiments were carried out at room temperature under dry conditions in transmission geometry, as shown in Figure 3. The fundamental light was the linearly polarized output of a mode-locked Ti:sapphire laser (Coherent Mira Seed, oscillator-only) pumped by an Ar ion laser (Coherent Innova 318): nominally 50 fs wide, ~4.5 nJ energy, laser pulses at 76 MHz repetition rate. The fundamental wavelength was set at 840 nm. This wavelength was chosen for the fundamental because, due to the presence of the broad B-band (Soret) that peaked at 425 nm,[7] the SHG signal at 420 nm should be resonantly enhanced. However, the available hyper-Rayleigh scattering (HRS) data for the **RuPZn** indicates that for this chromophore the magnitude of β_λ exhibits a substantial frequency dispersion; note that β_λ values for **RuPZn** determined at incident irradiation wavelengths in the 800 nm region are much smaller than those determined at longer wavelengths. The theoretical basis for this experimental observation has been recently provided.[22] The oscillator-only femtosecond laser was used, since in nonlinear optical experiments a high peak power is needed while low pulse energy minimizes heating and photochemical effects. The laser beam was directed to the sample using a combination of three silver-coated mirrors. The linear polarization of the incident beam was controlled by a rotating $\lambda/2$ plate. Any spurious second harmonic contribution from the optics was removed by means of a long pass filter F1 (Schott RG695) with cutoff at ~700 nm. A 20 cm focal length lens was chosen in order to narrow the laser beam waist from ~1 mm to ~200 μm and increase the peak intensity to ~100 MW/cm^2. The choice of this focusing lens was dictated by the need of having a strong SH signal without photochemically damaging the sample over time. The sample was mounted on a rotation stage that can also be translated in the $x-y$ directions so that the sample position could be adjusted with respect to the focal point. The angle of the incident beam was chosen to be 60° with respect to the surface normal. The beam transmitted through the sample was filtered with a band-pass filter (Schott BG39), passing band 330−600 nm, in order to filter out any contribution from the fundamental light. A rotating polarizer, with extinction coefficient of 1×10^{-5}, was used to select the output *p*- or *s*-polarization. A second band-pass filter (Schott BG39) was used to filter out any contribution given by the polarizer. Finally, the beam was collimated with a 10 cm focal length lens into the monochromator (Jarrel-Ash 1/4 m). The monochromator had, at both entrance and exit, a 1 mm slit, and was set at 420 nm with a 2 nm bandwidth. The signal was then detected by a photomultiplier, amplified, and then processed through a correlated photon counting system before being sent to the RS232 acquisition board. In each experiment, the SH intensity at each fundamental polarization angle was averaged over five points measured for 1 s each.

IV. Results

There are several potential sources for the SH signal in the sample: these include the interface between any two media or from the molecular film. It is known that peptides can be good SH and SF (sum-frequency) generators.[47−50] Therefore, experiments were conducted to determine if SH light could be generated from the **AP0** peptides or sources other than the chromophore molecules. Negligible SH signal was detected from the peptide monolayer before the incorporation of the **RuPZn** chromophores. The SH signals measured for a single monolayer of the **AP0** peptide deposited at a surface area corresponding to 100 Å^2 per helix before and after incorporation of the **RuPZn** chromophore are shown in Figure 4 for comparison. These data confirm that the detected SH signal derives as anticipated from the **RuPZn** chromophore in the peptide monolayer. In Figure 4 both *p*- and *s*-polarized SH intensity are reported as transmitted from the substrate as a function of the polarization angle of the incoming fundamental beam. The data shown are the average of measurements on different areas of a sample whose chromophore in-plane density was estimated from UV−vis absorption experiments to be ~6.7×10^{13} cm^{-2}.[34]

The SH intensity from samples with different in-plane chromophore densities was found to scale as the square of the in-plane density as expected for coherent SHG from arrays of orientationally ordered chromophores. In Figure 5 the *p*- and *s*-polarized SH intensity for incident polarization $\gamma = 0$ and 45°, respectively, are reported for different samples as a function

(47) Vogel, V.; Smiley, B. L. In *Laser Study of Macroscopic Biosystems*; 1st ed.; SPIE: Jyvaskyla, Finland, 1993; Vol. 1922, p 86.
(48) Chen, X. Y.; Wang, J.; Sniadecki, J. J.; Even, M. A.; Chen, Z. *Langmuir* **2005**, *21*, 2662.
(49) Chen, X.; Boughton, A. P.; Tesmer, J. J. G.; Chen, Z. *J. Am. Chem. Soc.* **2007**, *129*, 12658.
(50) Gualtieri, E. J.; Haupert, L. M.; Simpson, G. J. *Chem. Phys. Lett.* **2008**, *465*, 167.

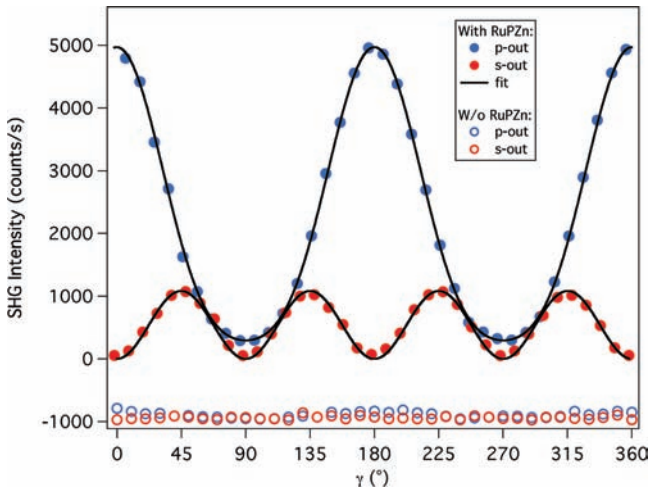

Figure 4. Polarized (*p*, blue; *s*, red) SH intensities versus the fundamental polarization angle for a single monolayer film of the **AP0** peptide covalently attached to the surface of a fused silica substrate before (empty circles) and after (filled circles) incorporation of the **RuPZn** chromophore (in-plane density $\sim 6.7 \times 10^{13}$ cm^{-2}). The solid lines indicate the best fit to the experimental data. For clarity the experimental data of the **AP0** peptide monolayer before incorporation of the **RuPZn** chromophore have been offset to -1000 count/s.

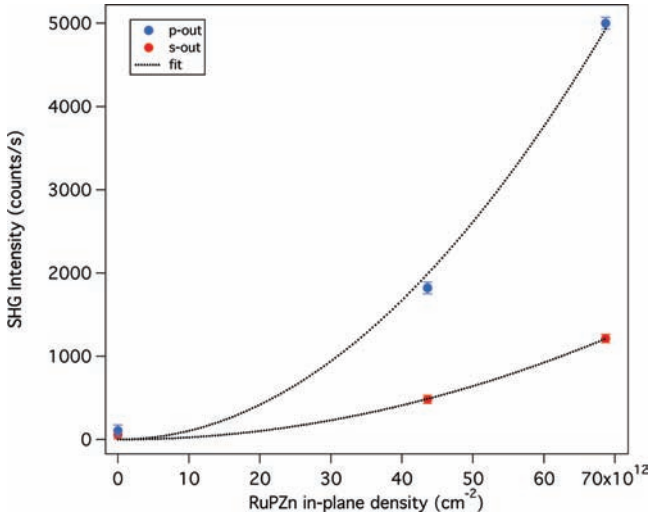

Figure 5. Polarized (*p*, blue; *s*, red) SH intensity, at incident polarization angles $\gamma = 0$ and 45°, respectively, where the maximum intensity is detected, as a function of the **RuPZn** in-plane density. The dotted lines are fits to a function proportional to the square of the in-plane chromophore density.

of their in-plane chromophore density, after averaging on different areas of each sample. The dotted lines represent the fit of the data to a function $f(N) = aN^2$, where a is a constant and N indicates the **RuPZn** in-plane density as in eq 6 for a coherent process.

V. Theoretical Analysis and Discussion

On the basis of the experimental observations it is clear that the SH signal originates from the interaction of light with the hyperpolarizable **RuPZn** chromophores embedded in the peptide monolayer: the peptide serves to only support and orient the **RuPZn** chromophores.

In order to obtain information about the nonlinear optical properties and orientation of the chromophores in the monolayer at high chromophore density, the experimental data in Figure 4 have been fitted to eq 2 (continuous lines) according to the theory reported above. The values used for the refractive indexes in the fitting procedure are the following: $n_1^{\omega} = n_1^{2\omega} = 1$ for air, $n_2^{\omega} = 1.45$ and $n_2^{2\omega} = 1.47$ for the fused silica substrate, and $n_3^{\omega} = 1.59$ and $n_3^{2\omega} = 1.59 + \mathrm{i}\ 0.13$ for the nonlinear monolayer. The real part of the refractive index of the monolayer composed of **AP0** peptides and **RuPZn** chromophores was obtained from the Bruggeman effective medium approximation considering a 10% of the volume occupied by the **RuPZn**, with refractive index 2.00 for the dense chromophore, and 90% occupied by the peptide with refractive index 1.55 (the same value of 1.59 is obtained using Maxwell-Garnett effective medium approximation).[51] The imaginary part, k, was obtained from the analysis of the UV−vis data[34] at the fundamental and SH wavelengths and calculated as $k = (\lambda A_{OD} \ln(10))/(4\pi d)$, where λ is the wavelength, A_{OD} the optical density, and d the film thickness. For the substrate the refractive index of pure fused silica was used. The alkylated layer present on the surface of the silica substrate is generally considered as having a refractive index in the visible ranging between 1.45 and 1.50,[52,53] very similar to that of silica, so its contribution can be disregarded.

A nonlinear least-squares fit, using eqs 2−5, to the data in Figure 4 results in $\chi_{zzz}/\chi_{xzx} = 3.3 \pm 0.3$ and $\chi_{zxx}/\chi_{xzx} = 0.4 \pm 0.1$. The fit to a second-order equation produces two sets of solutions but only the one physically meaningful is reported here. On the basis of comparisons of the SH intensity measured from our sample with that from a Y-cut quartz single crystal,[54] the absolute magnitude of the $\vec{\vec{\chi}}^{S}$, or equivalently the $\vec{\vec{\chi}}^{S,eff}$, elements can be obtained. The *p*-polarized SH intensity from quartz, using *p*-polarized fundamental at normal incidence, and the *s*-polarized SH intensity from our sample, generated with a 45°-polarized fundamental at 60° incidence, were used for the comparison. In this analysis, the thickness of the nonlinear monolayer and the coherence length of light in quartz, in addition to the appropriate Fresnel coefficients, were also taken into account. The coherence length, calculated from the phase-matching condition, for the quartz crystal is 4200 nm. As this length is much shorter than the other dimensions of consideration, such as the length of the laser focus region and the laser pulse width, it is used to account for the effective length for SHG in quartz. The effective length of the nonlinear monolayer has been obtained by correcting the thickness (6.3 nm) for the angle of incidence. From this comparison a value for $|\chi_{zxx}| = (4.6 \pm 0.1) \times 10^{-9}$ is obtainable which, with the previously determined ratios among the susceptibility tensor elements, results in $|\chi_{zxx}| = (1.9 \pm 0.4) \times 10^{-9}$ and $|\chi_{zzz}| = (15.2 \pm 1.3) \times 10^{-9}$ esu. In the comparison, a value of 1.9×10^{-9} esu, or 0.8 pm/V, for the χ_{xxx} of quartz was used. This value for the quartz susceptibility was originally obtained for a fundamental wavelength of 1.0582 μm:[56] in this work this same value has been used for 840 nm, since little variation is expected for the χ_{xxx} value between these two wavelengths.[57,58]

(51) Choy, T. C. *Effective Medium Theory: Principles and Applications*; Oxford University Press: New York, 1999.
(52) Ulman, A. *An Introduction to Ultrathin Organic Films: from Langmuir-Blodgett to Self-Assembly*; Academic Press: Boston, 1991.
(53) Gonella, G.; Cavalleri, O.; Emilianov, I.; Mattera, L.; Canepa, M.; Rolandi, R. *Mater. Sci. Eng. C* **2002**, *22*, 359.
(54) Ashwell, G. J.; Hargreaves, R. C.; Baldwin, C. E.; Bahra, G. S.; Brown, C. R. *Nature* **1992**, *357*, 393.
(55) Balzer, F.; Shamery, K. A.; Neuendorf, R.; Rubahn, H. G. *Chem. Phys. Lett.* **2003**, *368*, 307.
(56) Pressley, R. J.; Chemical Rubber Company. *CRC Handbook of Lasers, with Selected Data on Optical Technology*; Chemical Rubber Co.: Cleveland, 1971.

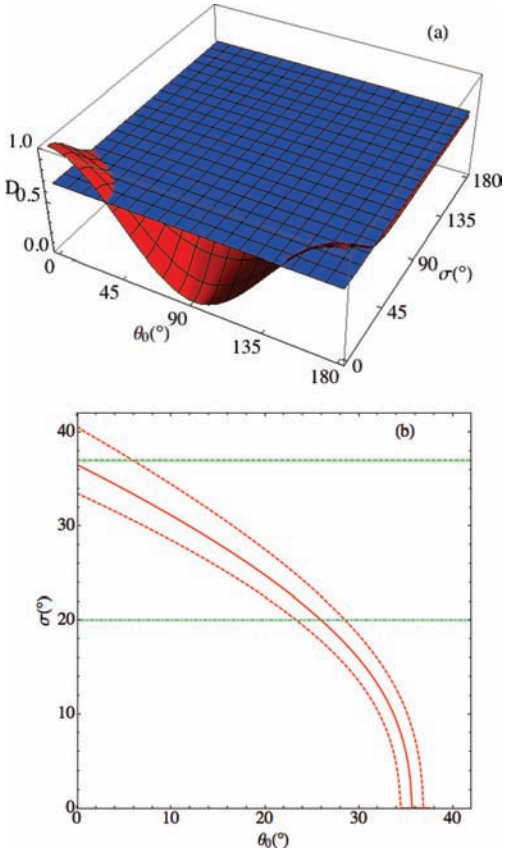

Figure 6. (a) Graphical solution to eq 9 for $D = 0.66$ using a normalized and truncated Gaussian distribution. (b) Locus of the pairs (θ_0, σ) satisfying $D = 0.66$ (red continuous line), as well as 0.64 and 0.68 (red dashed lines). The green lines represent $\sigma = 37°$ (dashed) and $\sigma = 20°$ (dash-dotted), respectively.

From the values of the $\vec{\vec{\chi}}^{S}$ elements obtained from the fit $D = 0.66 \pm 0.02$ and $(\beta_{z'x'x'} + \beta_{z'y'y'})/\beta_{z'z'z'} = -0.22 \pm 0.04$ were deduced. The value obtained for the ratio $(\beta_{z'x'x'} + \beta_{z'y'y'})/\beta_{z'z'z'}$ is in good agreement with the fact that for push−pull chromophores the $\beta_{z'z'z'}$ element of the hyperpolarizability tensor is considered as the dominant one.

Once the value of D is known from the susceptibility elements, it is possible to identify all the values for the pair of parameters (θ_0, σ) characterizing the distribution function of the tilt angle. In Figure 6a the graphical solution of the equation $\langle \cos^3\theta \rangle / \langle \cos\theta \rangle = 0.66$ is reported: the pairs (θ_0, σ) belonging to both the $\langle \cos^3\theta \rangle / \langle \cos\theta \rangle$ surface (red in Figure 6a) and the plane at $D = 0.66$ (blue in Figure 6a) are the set of possible solutions to the equation. The symmetry of the solution with respect to $\theta_0 = 90°$ reflects the fact that SHG is sensitive to the angle of the dipole with respect to the normal to the surface, but not to its direction. Note that for the tilt angle a particular θ_0 is equivalent to $(180° - \theta_0)$ we, therefore, now restrict our attention to the [0°,90°] range. The set of solutions for the tilt angle and distribution width is plotted in Figure 6b. The possible set of parameters range from ($\theta_0 = 0°$, $\sigma = (36.5^{+4.0}_{-3.0})°$) to ($\theta_0 = (35.7 \pm 1.2)°$, $\sigma = 0°$). Once the pairs (θ_0, σ) satisfying $D = 0.66$ are known, it is possible to obtain the corresponding values of $|\beta_{z'z'z'}|$.

As shown in Figure 7, a value of $\sim 300 \times 10^{-30}$ esu is found. This value for the **RuPZn** molecular hyperpolarizability obtained at incident laser irradiation wavelength of 840 nm is in good agreement with that measured in HRS experiments of the chromophore in isotropic solution[7] where values $<50 \times 10^{-30}$ esu at 800 nm and 2100×10^{-30} esu at 1064 nm were reported. It is important to note as well that the $|\beta_{z'z'z'}|$ (β_{840}) value of $\sim 300 \times 10^{-30}$ esu derived from these SHG data is also in close agreement with that computed at this wavelength using a theoretical analysis that exploits generalized Thomas−Kuhn sum rules, experimental linear absorption data, and measured hyperpolarizabilities at multiple frequencies to compute the entire frequency-dependent electronic hyperpolarizability spectrum.[22] Comparisons of these experimental and computed β_λ values thus suggest that the incorporation of the chromophore in the bundle does not influence the chromophore NLO response and that the chromophore−chromophore interactions in the densely packed ensemble are small enough not to substantially affect the molecular hyperpolarizability. This is particularly important given that the experimental hyperpolarizability determined for **RuPZn** at a telecommunications-relevant wavelength (1300 nm) is more than an order of magnitude larger than this $|\beta_{z'z'z'}|$ value determined at 840 nm.[7]

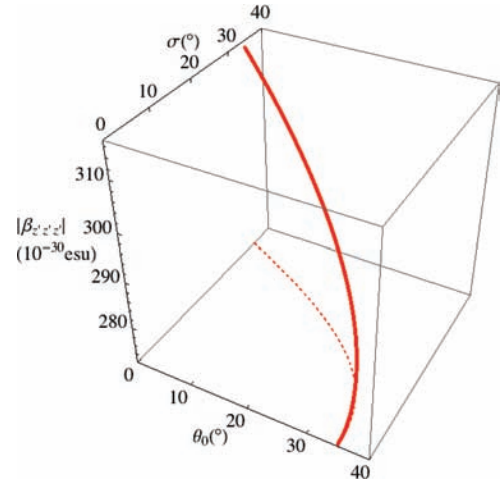

Figure 7. The values of the $z'z'z'$ component of the first-order hyperpolarizability for the pairs (θ_0, σ) satisfying $D = 0.66$ (solid line). The dashed line represents the $|\beta_{z'z'z'}|$ projection on the (θ_0, σ) plane.

The width and the center of the tilt angle distribution are entangled and it has been shown that assuming a narrow angular distribution may be misleading.[59] From our data analysis the set of possible solutions for the tilt angle distribution is shown in red in Figure 6b. This interdependence may be at least partially resolved by applying some physical considerations. First, grazing-incidence X-ray diffraction (GIXD) from the precursor Langmuir monolayer of **AP0** (apo) indicates that while the average orientation of the 4-helix bundle axis is perpendicular to the plane of the water−gas interface, the width of the orientational distribution of the bundle axis over the monolayer ensemble might be quite large (Figure 6 in ref 34). Treating the helices in the bundle as simple solid cylinders provides an upper estimate for this width such that $\sigma \leq 37°$ (green dashed line in Figure 6b). Given that molecular dynamics (MD) simulations for a similar chromophore indicated that the chromophore long-axis was highly aligned along the axis of the bundle,[33] this upper limit for the width of the tilt angle distribution of the tightly coupled **AP0**−**RuPZn** bundle would

(57) Huang, M. Z.; Ching, W. Y. *Ferroelectrics* **1994**, *156*, 105.
(58) Hagimoto, K.; Mito, A. *Appl. Opt.* **1995**, *34*, 8276.
(59) Simpson, G. J.; Rowlen, K. L. *J. Am. Chem. Soc.* **1999**, *121*, 2635.

then result in a mean value of $\theta_0 \leq 6°$ for the tilt angle distribution. However, modeling the bundle as solid cylinders is an oversimplification, knowing that the helices tilt with respect to the bundle axis forming a coiled-coil structure. In fact, the pitch angle of ~20° determined from the GIXD characterizing this coiled-coil structure would already account for at least half of the estimated width from the simplistic model.[32,60] Thus, it seems more likely that the width of the tilt-angle distribution for the tightly coupled **AP0**−**RuPZn** bundle is actually relatively narrow, namely, $\sigma \leq 20°$ (green dash-dotted line in Figure 6b), resulting in the mean of the distribution being relatively larger than that indicated by the simplistic model, namely, $23° \leq \theta_0 \leq 37°$ from Figure 6b. This is not so unreasonable given that the **AP0** (apo) in the precursor Langmuir monolayer, under an applied surface pressure that aligns the bundle axis perpendicular to the interface, was covalently attached to the surface of the fused silica substrate and subsequently removed from the Langmuir trough, thereby releasing this surface pressure constraint. Unfortunately, GIXD measurements that could potentially provide this mean value are then no longer possible on the Langmuir−Schaefer monolayer due to the high background scattering from the underlying amorphous silica substrate.

VI. Concluding Remarks

A new "directed assembly" approach (described in ref 34) has proven successful for the fabrication of a new class of nonlinear optical materials. In particular, this approach is based on incorporating a benchmark, highly hyperpolarizable nonlinear optical chromophore (**RuPZn**) into a monolayer ensemble of a designed artificial 4-helix bundle peptide (**AP0**) at high in-plane density on a silica substrate. This fabrication technique has proven effective for the translation of the microscopic nonlinear properties of the chromophore to the macroscopic scale. The artificial peptide is used to control both the orientational order of the chromophore molecules within the bundle and their positions within a monolayer ensemble in the absence of an applied external field; this approach stands in sharp contrast to the common guest−host electric field poling strategy that has been utilized extensively to prepare NLO materials based on soft matter chromophore/polymer components. This peptide-based method provides optimal control of the chromophore orientational and positional ordering with high in-plane chromophore densities and ensures a large macroscopic susceptibility for a single monolayer in the linear response regime. These **AP0**−**RuPZn** monolayer samples have proven to be reasonably robust for an organic material and thereby potentially suitable for nonlinear optical device applications, as they are stable in air indefinitely and capable of withstanding relatively intense laser irradiation (e.g., peak power per unit surface of ~100 MW/cm^2), although some degradation in the SHG signal was observed under such continuous irradiation over the time scale of an hour.

Acknowledgment. G.G. and H.L.D. acknowledge the National Science Foundation GOALI grant #0616836 for support of the NLO measurements. They also thank Miss Jia Zeng for assistance with the laser system and Prof. Garth J. Simpson for discussions on the derivation of the Fresnel factors. M.J.T., H.C.F., V.K., and J.K.B. acknowledge primary support from the Department of Energy Biomolecular Materials grant DE-FG02-94ER46156 and partial support (A.T. and J.K.B.) from the National Science Foundation MRSEC grant DMR05-20029 and NSEC grant DMR-0425780.

Supporting Information Available: A detailed derivation of the L^{Ω} ($\Omega = \omega, 2\omega$) factors is presented. This material is available free of charge via the Internet at http://pubs.acs.org.

JA1010724

(60) Zou, H.; Strzalka, J.; Xu, T.; Tronin, A.; Blasie, J. K. *J. Phys. Chem. B* **2007**, *111*, 1823.